

Solvothermal Synthesis and Structure of Ni(HP₂O₇)F·C₂N₂H₁₀, a New Fluorinated Nickel Phosphate with a Chain Structure

Yunling Liu, Lirong Zhang, Zhan Shi, Hongming Yuan, and Wenqin Pang¹*Key Laboratory of Inorganic Synthesis and Preparative Chemistry, Jilin University, Changchun 130023, China*

Received September 26, 2000; in revised form November 14, 2000; accepted December 8, 2000; published online March 8, 2001

A new one-dimensional fluorinated nickel phosphate Ni(HP₂O₇)F·C₂N₂H₁₀ has been synthesized solvothermally using ethylenediamine as the template and its structure was determined by means of single-crystal X-ray diffraction. The title compound crystallizes in the monoclinic system, space group *C*/2*c* (No. 15) with *M* = 314.78, *a* = 12.658(3) Å, *b* = 14.502(3) Å, *c* = 10.820(3) Å, β = 109.924(5)°, *V* = 1867.3(8) Å³, *Z* = 8, *R* = 0.0318, and *wR* = 0.0670. The structure consists of infinite chains of *cis*, *trans*-corner-sharing NiO₄F₂ octahedra with the adjacent octahedra being bridged by HP₂O₇ groups, which are H-bonded with amine groups of the organic cations. The Ni–F bond lengths along the backbone of the chain are alternately short and long. The as-synthesized product is characterized by powder X-ray diffraction, IR spectroscopy, inductive couple plasma analysis, thermogravimetric analysis, and differential thermal analysis. © 2001 Academic Press

Key Words: solvothermal synthesis; structure; nickel phosphate; chain.

INTRODUCTION

Considerable efforts have been made during the past decade to prepare open-framework metal phosphates that may find applications in catalysis, adsorption, ionic conduction, ion-exchange, electronics, and optoelectronics. Since the discovery of the microporous crystalline aluminophosphates (1), a large number of new metal phosphates with open frameworks have appeared in the literature, and the metals include gallium (2), indium (3), zinc (4), iron (5), tin (6), titanium (7), vanadium (8), and molybdenum (9). However, reports about nickel phosphates are few, and only several nickel phosphate VSB-*m* (*m* = 1–4) compounds with an open framework (10, 11) and some alkali-metal nickel phosphates (12–18) (most of them were prepared by solid-state reactions) have been reported. To our knowledge,

organically templated nickel phosphate has not yet been discovered. In the past decade, the nonaqueous techniques and the fluoride method have been used successfully for the synthesis of ultralarge pore molecular sieves JDF-20 (19) and cloverite (20), and other known or novel 1-D, 2-D, and 3-D structural materials (21). Therefore, solvothermal synthesis has proved to be an exciting and promising method to prepare materials with new structures (22).

In this paper we report the solvothermal synthesis and X-ray structural characterization of a new fluorinated nickel phosphate Ni(HP₂O₇)F·C₂N₂H₁₀, using ethylenediamine as the organic structure-directing agent in a fluoride-containing system.

EXPERIMENTAL

Synthesis and Characterization

The title compound was prepared solvothermally from a mixture of nickel acetate (Ni(CH₃COO)₂·4H₂O, 98%), phosphoric acid (H₃PO₄, 85 wt%), triethylene glycol (TEG), ethylenediamine (en, 99%), and hydrofluoric acid (HF, 40%) with the molar ratio 1.0 Ni(CH₃COO)₂·4H₂O:2.0 H₃PO₄:4.0 TEG:2.0 en:2.0 HF. Typically, 0.6 g of nickel acetate was first dispersed into 13 ml of triethylene glycol with stirring, and then 0.3 ml of H₃PO₄ and 0.4 ml of HF were added successively with stirring to form a clear solution. Finally, 0.3 ml of ethylenediamine was added dropwise under vigorous stirring. The gel thus formed was stirred until homogenous. The final mixture was sealed in a Teflon-lined stainless-steel autoclave and heated at 453 K for 14 days under autogenous pressure. The product (in about 80% yield based on the Ni source) consisting of greenish yellow cubic crystals was recovered by filtration, washed thoroughly with distilled water, and dried at room temperature.

Powder X-ray diffraction (XRD) data were collected on a Siemens D5005 diffractometer with CuKα radiation (λ = 1.5418 Å). The step size was 0.02° and the count time was 4 s. The elemental analyses were performed on a Perkin-Elmer 240C element analyzer. Inductively coupled

¹To whom correspondence should be addressed. Fax: +86-431-5671974. E-mail: wqpang@mail.jlu.edu.cn.



TABLE 1
Crystal Data and Structure Refinement
for Ni(HP₂O₇)F · C₂N₂H₁₀

Empirical formula	C ₂ H ₁₁ FN ₂ NiO ₇ P ₂
Formula weight	314.78
Temperature	293(2) K
Wavelength	0.71073 Å
Crystal system	Monoclinic
Space group	C2/c
Unit cell dimensions	$a = 12.658(3) \text{ \AA}$, $\alpha = 90^\circ$ $b = 14.502(3) \text{ \AA}$, $\beta = 109.924(5)^\circ$ $c = 10.820(3) \text{ \AA}$, $\gamma = 90^\circ$
Volume	1867.3(8) Å ³
Z	8
Density (calculated)	2.239 Mg/m ³
Absorption coefficient	2.458 mm ⁻¹
F(000)	1280
Crystal size	0.08 × 0.08 × 0.08 mm ³
θ range for data collection	2.21–23.27°
Limiting indices	$-13 \leq h \leq 14$, $-16 \leq k \leq 9$, $-12 \leq l \leq 12$
Reflections collected/unique	4472/1339 [$R(\text{int}) = 0.0469$]
Completeness to $\theta = 23.27$	99.9%
Refinement method	full-matrix least-squares on F^2
Data/restraints/parameters	1339/6/182
Goodness-of-fit on F^2	0.988
Final R indices [$I > 2\sigma(I)$]	$R_1 = 0.0318$, $wR_2 = 0.0670$
R indices (all data)	$R_1 = 0.0492$, $wR_2 = 0.0716$
Largest diff. peak and hole	0.445 and $-0.437 \text{ e} \cdot \text{ \AA}^{-3}$

plasma (ICP) analysis was carried out on a Perkin-Elmer Optima 3300DV ICP instrument. The infrared (IR) spectrum was recorded within the 400–4000 cm⁻¹ region on a Nicolet Impact 410 FTIR spectrometer using KBr pellets. A Perkin-Elmer DTA 1700 differential thermal analyzer was used to obtain the differential thermal analysis (DTA),

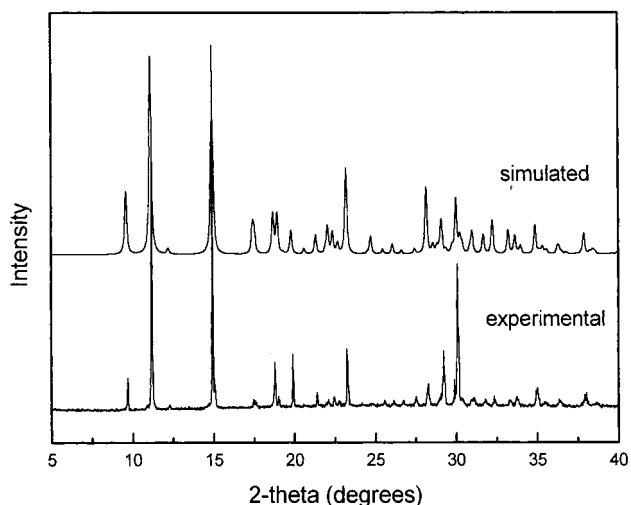


FIG. 1. Experimental and simulated powder X-ray diffraction patterns of Ni(HP₂O₇)F · C₂N₂H₁₀.

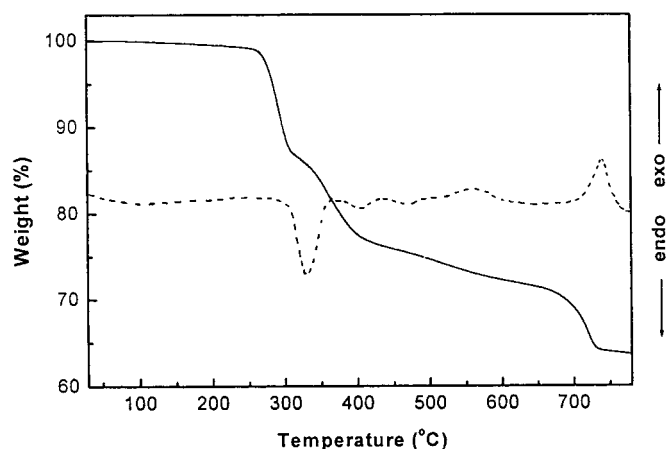


FIG. 2. TGA (—) and DTA (---) curves for Ni(HP₂O₇)F · C₂N₂H₁₀.

and a Perkin-Elmer TGA 7 thermogravimetric analyzer was used to obtain thermogravimetric analysis (TGA) curves in an atmospheric environment with a heating rate of 20°C min⁻¹.

TABLE 2
Atomic Coordinates ($\times 10^4$) and Equivalent Isotropic Displacement Parameters ($\text{\AA}^2 \times 10^3$) for Nonhydrogen Atoms and Isotropic Displacement Parameters ($\text{\AA}^2 \times 10^3$) for Hydrogen Atoms for Ni(HP₂O₇)F · C₂N₂H₁₀

	x	y	z	U(eq)
Ni(1)	2500	-2500	5000	15(1)
Ni(2)	0	-1489(1)	2500	16(1)
P(1)	2399(1)	-1646(1)	2314(1)	17(1)
P(2)	2145(1)	-392(1)	4250(1)	17(1)
F	840(2)	-2442(2)	3857(2)	22(1)
O(1)	3134(3)	-1587(2)	1457(3)	24(1)
O(2)	2826(3)	-2425(2)	3271(3)	21(1)
O(3)	1165(3)	-1648(2)	1527(3)	21(1)
O(4)	2644(3)	-694(2)	3117(3)	21(1)
O(5)	2584(3)	-1076(2)	5353(3)	21(1)
O(6)	873(2)	-415(2)	3653(3)	20(1)
O(7)	2617(3)	569(2)	4537(3)	25(1)
N(1)	5316(4)	6213(3)	1155(5)	30(1)
N(2)	4030(4)	1197(3)	3073(5)	30(1)
C(1)	4778(5)	6895(4)	1762(5)	26(1)
C(2)	4788(6)	438(5)	3058(8)	47(2)
H(1)	2970(60)	-1200(40)	900(60)	70(20)
H(1NA)	5150(50)	5640(30)	1300(60)	50(20)
H(1NB)	6030(30)	6350(40)	1350(60)	60(20)
H(1NC)	4980(60)	6280(50)	300(40)	100(30)
H(2NA)	3610(40)	1370(30)	2290(40)	35(17)
H(2NB)	3560(40)	1100(40)	3550(50)	60(20)
H(2NC)	4400(40)	1720(30)	3340(40)	26(15)
H(1CA)	4950(40)	7450(30)	1390(40)	15(12)
H(1CB)	4020(40)	6810(30)	1470(40)	25(14)
H(2CA)	4430(50)	-120(50)	3200(50)	70(20)
H(2CB)	5300(60)	460(50)	3730(70)	80(30)

Note. U(eq) is defined as one-third of the trace of the orthogonalized U_{ij} tensor.

TABLE 3
Selected Bond Lengths (Å) and Angles (°)
for Ni(HP₂O₇)F · C₂N₂H₁₀

Ni(1)–F	2.044(2)	Ni(2)–F # 2	2.034(2)
Ni(1)–F # 1	2.044(2)	Ni(2)–F	2.034(2)
Ni(1)–O(2) # 1	2.051(3)	Ni(2)–O(6)	2.065(3)
Ni(1)–O(2)	2.051(3)	Ni(2)–O(6) # 2	2.065(3)
Ni(1)–O(5) # 1	2.096(3)	Ni(2)–O(3) # 2	2.096(3)
Ni(1)–O(5)	2.096(3)	Ni(2)–O(3)	2.096(3)
P(1)–O(3)	1.503(3)	P(2)–O(5)	1.505(3)
P(1)–O(2)	1.503(3)	P(2)–O(7)	1.506(3)
P(1)–O(1)	1.524(4)	P(2)–O(6)	1.517(3)
P(1)–O(4)	1.604(3)	P(2)–O(4)	1.619(3)
N(1)–C(1)	1.477(7)	C(1)–C(1) # 3	1.502(10)
N(2)–C(2)	1.464(8)	C(2)–C(2) # 3	1.479(14)
F–Ni(1)–F # 1	180.00(18)	F–Ni(2)–O(6)	92.06(11)
F–Ni(1)–O(2) # 1	93.97(11)	F # 2–Ni(2)–O(6) # 2	92.06(11)
F # 1–Ni(1)–O(2) # 1	86.03(11)	F–Ni(2)–O(6) # 2	171.76(11)
F–Ni(1)–O(2)	86.03(11)	O(6)–Ni(2)–O(6) # 2	82.09(16)
F # 1–Ni(1)–O(2)	93.97(11)	F # 2–Ni(2)–O(3) # 2	90.21(11)
O(2) # 1–Ni(1)–O(2)	180.0	F–Ni(2)–O(3) # 2	81.17(11)
F–Ni(1)–O(5) # 1	87.29(11)	O(6)–Ni(2)–O(3) # 2	95.92(12)
F # 1–Ni(1)–O(5) # 1	92.71(11)	O(6) # 2–Ni(2)–O(3) # 2	93.61(12)
O(2) # 1–Ni(1)–O(5) # 1	95.79(12)	F # 2–Ni(2)–O(3)	81.17(11)
O(2)–Ni(1)–O(5) # 1	84.21(12)	F–Ni(2)–O(3)	90.21(11)
F–Ni(1)–O(5)	92.71(11)	O(6)–Ni(2)–O(3)	93.61(12)
F # 1–Ni(1)–O(5)	87.29(11)	O(6) # 2–Ni(2)–O(3)	95.92(12)
O(2) # 1–Ni(1)–O(5)	84.21(12)	O(3) # 2–Ni(2)–O(3)	167.35(18)
O(2)–Ni(1)–O(5)	95.79(12)	O(3)–P(1)–O(2)	116.70(19)
O(5) # 1–Ni(1)–O(5)	180.00(16)	O(3)–P(1)–O(1)	112.81(19)
F # 2–Ni(2)–F	94.32(14)	O(2)–P(1)–O(1)	108.11(19)
F # 2–Ni(2)–O(6)	171.76(11)	O(3)–P(1)–O(4)	106.27(18)
O(2)–P(1)–O(4)	108.42(17)	Ni(2)–F–Ni(1)	129.90(13)
O(1)–P(1)–O(4)	103.63(19)	P(1)–O(1)–H(1)	116(5)
O(5)–P(2)–O(7)	115.71(18)	P(1)–O(2)–Ni(1)	122.08(18)
O(5)–P(2)–O(6)	112.00(19)	P(1)–O(3)–Ni(2)	119.22(17)
O(7)–P(2)–O(6)	113.38(19)	P(1)–O(4)–P(2)	126.2(2)
O(5)–P(2)–O(4)	106.75(18)	P(2)–O(5)–Ni(1)	121.54(16)
O(7)–P(2)–O(4)	100.17(18)	P(2)–O(6)–Ni(2)	123.10(18)
O(6)–P(2)–O(4)	107.59(17)	N(2)–C(2)–C(2) # 3	115.5(5)
N(1)–C(1)–C(1) # 3	114.2(5)		

Note. Symmetry transformations used to generate equivalent atoms: # 1, $-x + \frac{1}{2}, -y - \frac{1}{2}, -z + 1$; # 2, $-x, y, -z + \frac{1}{2}$; # 3, $-x + 1, y, -z + \frac{1}{2}$.

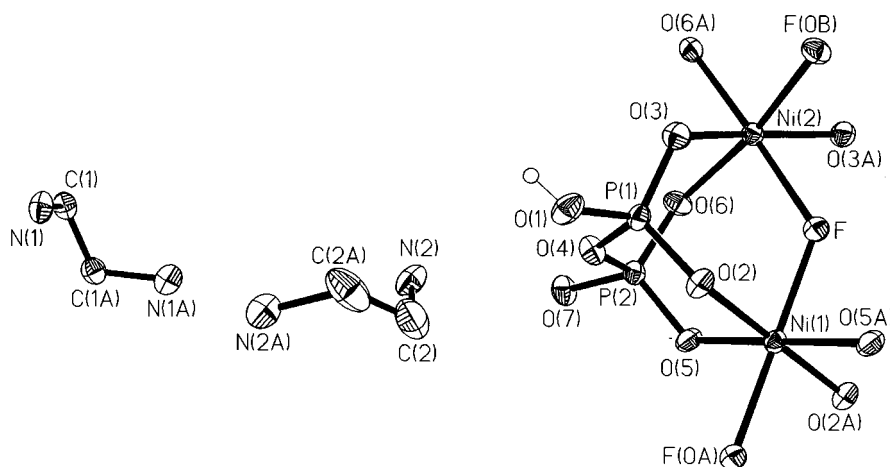


FIG. 3. ORTEP view of the Ni(HP₂O₇)F · C₂N₂H₁₀ structure showing the atom labeling scheme (50% thermal ellipsoids).

Determination of Crystal Structure

A greenish yellow cubic crystal of approximate dimensions $0.08 \times 0.08 \times 0.08 \text{ mm}^3$ was mounted on a glass fiber on a Bruker-AXS Smart CCD diffractometer equipped with a normal-focus, 2.4-kW sealed tube X-ray source (graphite-monochromated MoK α radiation, $\lambda = 0.71073 \text{ \AA}$) operating at 50 kV and 40 mA. Intensity data were collected in 1271 frames with increasing ω (width of 0.3° and exposure time of 30 s per frame). A total of 4472 reflections were collected at 293 K with 1339 unique reflections ($R_{\text{int}} = 0.0469$), of which 1044 were considered to be observed with $I > 2\sigma(I)$. Data processing was accomplished with the SAINT processing program (23). The structure was solved by direct methods and refined by full-matrix least-squares on F^2 using SHELXTL Version 5.1 (24). The nickel and phosphorus atoms were first located, and the carbon, nitrogen, fluorine, oxygen, and hydrogen atoms were found in the final difference Fourier map. All nonhydrogen atoms were refined anisotropically. The detailed crystallographic data are listed in Table 1.

RESULTS AND DISCUSSION

Synthesis

It is found that the use of solvothermal techniques and the involvement of fluoride ions are very essential in the formation of the title compound. If HF is omitted from the reaction mixtures, only amorphous nickel phosphate crystallizes. A new layered nickel phosphate product consisting of plate crystals is synthesized when NH₄F is used as the F⁻ source. In addition, the title compound cannot be prepared in an aqueous system.

Characterization

The ICP analysis for the title compound gives rise to a Ni/P ratio of $\frac{1}{2}$. The elemental analysis indicates that the

contents of C, H, and N are 7.84, 3.46, and 8.95%, respectively, in good agreement with the values (7.63, 3.50, and 8.90%) based on the single-crystal structure formula $\text{Ni}(\text{HP}_2\text{O}_7)\text{F} \cdot \text{C}_2\text{N}_2\text{H}_{10}$.

The powder X-ray diffraction pattern for $\text{Ni}(\text{HP}_2\text{O}_7)\text{F} \cdot \text{C}_2\text{N}_2\text{H}_{10}$ is entirely consistent with that simulated on the

basis of the single-crystal structure (Fig. 1). The diffraction peaks on both patterns correspond well in position, indicating the phase purity of the as-synthesized sample.

The IR spectrum of the compound shows the presence of vibrational bands characteristic of ethylenediamine at 1600, 1454, and 1308 cm^{-1} , and the intense bands at 1096 and

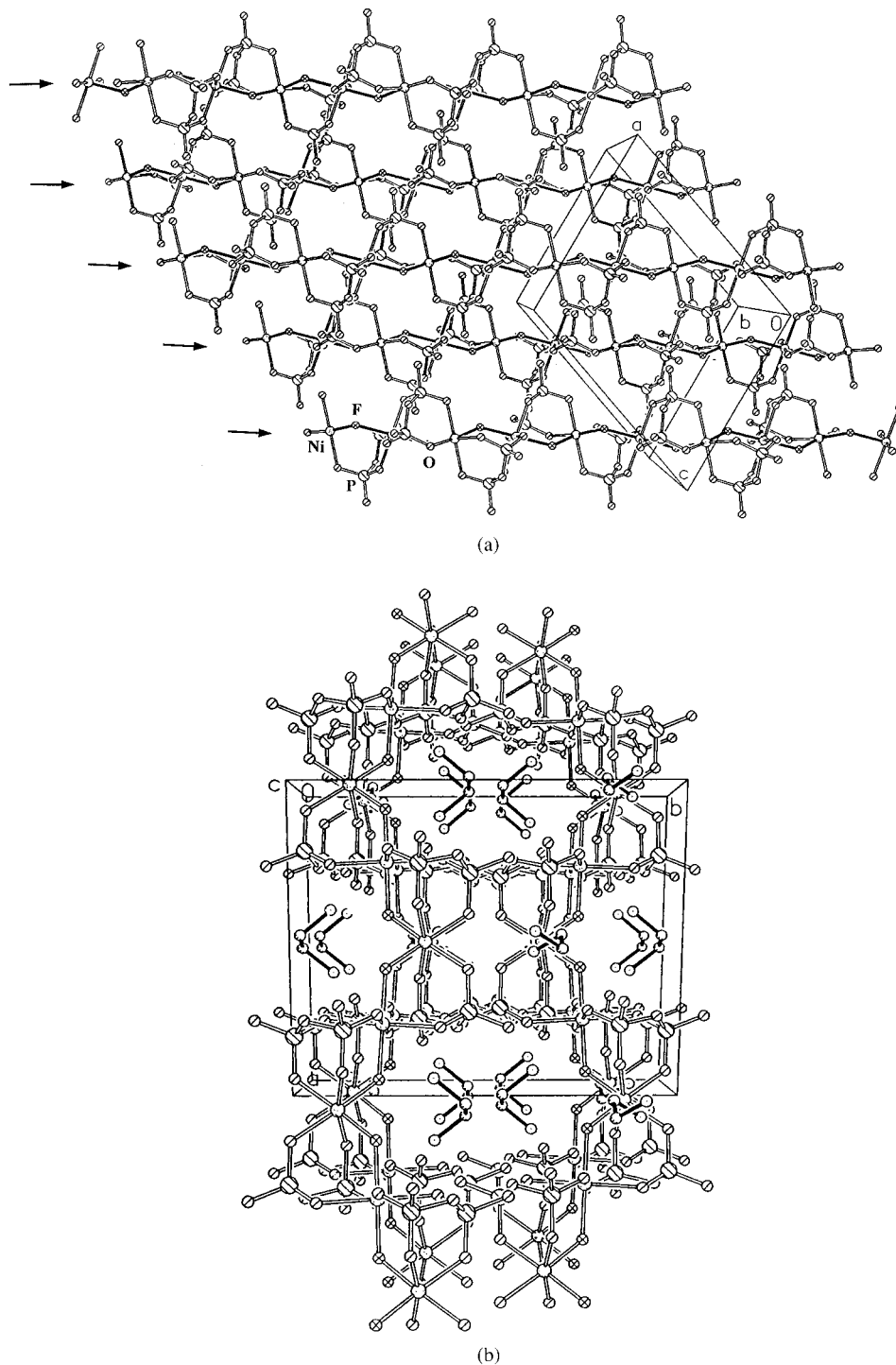


FIG. 4. (a) Structure of $\text{Ni}(\text{HP}_2\text{O}_7)\text{F} \cdot \text{C}_2\text{N}_2\text{H}_{10}$ viewed along the b -axis. The infinite chains are shown in the arrow direction (the $\text{Ni}-\text{F}-\text{Ni}$ bonds are represented by the black line and the organics have been omitted for clarity). (b) Structure of $\text{Ni}(\text{HP}_2\text{O}_7)\text{F} \cdot \text{C}_2\text{N}_2\text{H}_{10}$ viewed along the c -axis.

950 cm^{-1} are associated with the asymmetric stretching vibrations of phosphate groups. There appear absorptions at 615, 542, and 455 cm^{-1} as well due to bending vibrations of phosphate groups.

The thermogravimetric analysis (Fig. 2) shows that the weight loss of the compound is ca. 27.2% from 240 to 600°C, corresponding to the decomposition of the ethylenediamine template (calcd 19.7%) and HF molecule (calcd 6.35%), and the weight loss of 6.8% at 660–770°C is consistent with the dehydroxylation of the compound. The DTA curve exhibits one endothermic and one exothermic peak at ca. 327 and 745°C corresponding to the departure of the template and the dehydroxylation. The structure collapses and converts to an amorphous phase after calcination at 400°C for 2 hours. At 800°C, the resulting solid is the $\text{Ni}(\text{PO}_3)_2$ phase (JCPDS: 28-0708).

Description of the Structure

The final atomic coordinates, selected bond lengths, and bond angles are listed in Tables 2 and 3, respectively.

The structure consists of infinite macroanionic chains of empirical formula $[\text{Ni}(\text{HP}_2\text{O}_7)\text{F}]^{2-}$ separated by ethylenediamine cations. The atom-bonding scheme of $\text{Ni}(\text{HP}_2\text{O}_7)\text{F}$

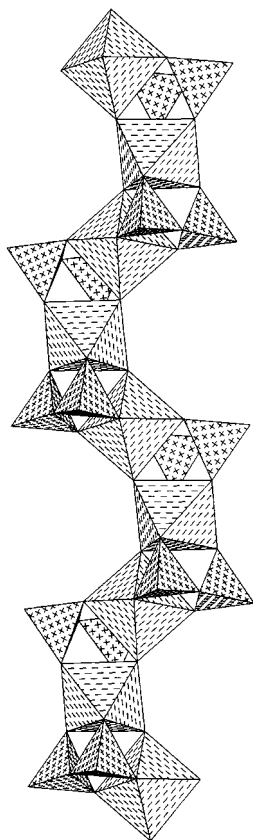


FIG. 5. Section of an infinite chain in $\text{Ni}(\text{HP}_2\text{O}_7)\text{F} \cdot \text{C}_2\text{N}_2\text{H}_{10}$.

$\text{C}_2\text{N}_2\text{H}_{10}$ is shown in Fig. 3. It contains two crystallographically different Ni atoms, two different P atoms, and one F atom. Two Ni atoms are at special positions and octahedrally coordinated by four oxygen atoms and two fluorine atoms with Ni–O distance from 2.051 to 2.096 Å and O–Ni–O bond angles in the range 82.09–180.00°. These results are close to those observed previously in nickel phosphates (14–18). The Ni atoms are linked together by *cis*, *trans*-coordinated F atoms to produce a zigzag Ni–F–Ni–F– backbone with alternating short and long Ni–F bonds (2.034 and 2.044 Å). Such alternation of the Ga–O and Al–O bond length along the chain axis has been observed in one-dimensional gallium phosphate (25) and the mineral overite (26). Two PO_4 tetrahedra form a P_2O_7 unit by corner-sharing, so one longer and three shorter P–O bonds are formed in each PO_4 tetrahedron. The P(1)–O(4)–P(2) angle is 126.2(2)°, which is in the range of those found in other diphosphates. The P_2O_7 unit has a hydroxy group (O(1)H(1) for HP_2O_7), and the H(1) atom was found in the difference Fourier map.

The structure of $\text{Ni}(\text{HP}_2\text{O}_7)\text{F} \cdot \text{C}_2\text{N}_2\text{H}_{10}$ consists of infinite $[\text{Ni}(\text{HP}_2\text{O}_7)\text{F}]_n^{2-}$ chains running parallel to the [101] direction (Fig. 4a). These chains are held together in a three-dimensional structure with the tunnel arranged in the *c* direction; in these tunnels the organic molecules are located (as shown in Fig. 4b). The NiO_4F_2 octahedra chains are linked in a *cis*–*trans* configuration (as shown in Fig. 5) in the same way as the titanyl chains in $\beta\text{-NaTiOPO}_4$ (27). Adjacent octahedra are bridged by the HP_2O_7 groups, via the sharing of four vertices of the HP_2O_7 groups. The cohesion of the structure is ensured by strong hydrogen bonds between the hydrogen atom H(1) of the HP_2O_7 groups and the terminal oxygen atoms O(7) of the neighbor-

TABLE 4
Hydrogen Bonds for $\text{Ni}(\text{HP}_2\text{O}_7)\text{F} \cdot \text{C}_2\text{N}_2\text{H}_{10}$

D–H ... A	<i>d</i> (D–H) (Å)	<i>d</i> (H ... A) (Å)	<i>d</i> (D ... A) (Å)	Angle (D–H ... A) (°)
O(1)–H(1) ... O(7) #4	0.80(6)	1.66(6)	2.449(4)	169(7)
N(1)–H(1NA) ... O(6) #5	0.88(3)	2.02(4)	2.846(6)	155(5)
N(1)–H(1NB) ... O(2) #6	0.87(4)	2.25(5)	2.970(6)	140(5)
N(1)–H(1NB) ... O(5) #7	0.87(4)	2.58(5)	3.275(6)	138(5)
N(1)–H(1NC) ... O(3) #8	0.88(4)	2.08(4)	2.937(6)	163(7)
N(2)–H(2NA) ... O(5) #4	0.87(3)	2.09(4)	2.894(6)	152(5)
N(2)–H(2NA) ... F #5	0.87(3)	2.36(5)	2.919(6)	122(4)
N(2)–H(2NA) ... O(2) #5	0.87(3)	2.44(5)	3.049(6)	127(4)
N(2)–H(2NB) ... O(7)	0.93(4)	2.00(4)	2.910(6)	166(5)
N(2)–H(2NC) ... F #9	0.88(3)	2.11(4)	2.922(6)	154(5)
N(2)–H(2NC) ... O(3) #5	0.88(3)	2.50(4)	3.176(6)	135(4)

Note. Symmetry transformations used to generate equivalent atoms:

#1, $-x + \frac{1}{2}$, $-y - \frac{1}{2}$, $-z + 1$; #2, $-x$, y , $-z + \frac{1}{2}$; #3, $-x + 1$, y , $-z + \frac{1}{2}$; #4, x , $-y$, $z - \frac{1}{2}$; #5, $-x + \frac{1}{2}$, $y + \frac{1}{2}$, $-z + \frac{1}{2}$; #6, $-x + 1$, $y + 1$, $-z + \frac{1}{2}$; #7, $x + \frac{1}{2}$, $-y + \frac{1}{2}$, $z - \frac{1}{2}$; #8, $-x + \frac{1}{2}$, $-y + \frac{1}{2}$, $-z$; #9, $x + \frac{1}{2}$, $y + \frac{1}{2}$, z .

ing HP₂O₇ groups with the distance of $d_{O(1)-H(1)\dots O(7)} = 2.449(4)\text{\AA}$. Furthermore, there are extensive hydrogen bonds among the bridging oxygens, fluorines, and the amine groups of the organic molecule, which contribute to the linkage of the nickel phosphate chains. Detailed information about the hydrogen bonding is summarized in Table 4.

CONCLUSION

A new fluorinated nickel phosphate has been prepared under solvothermal conditions in a fluoride-bearing system. We are continuing the exploratory synthesis of a new nickel phosphate by variation of template agent and crystallization conditions.

ACKNOWLEDGMENTS

The authors acknowledge the financial support from the State Basic Research Project of China (G200077507), the National Natural Science Foundation of China (29871012, 29733070), and the Key Laboratory of Inorganic Synthesis and Preparative Chemistry of Jilin University.

REFERENCES

1. S. T. Wilson, B. M. Lok, C. A. Messina, T. R. Cannan, and E. M. Flanigen, *J. Am. Chem. Soc.* **104**, 1146 (1982).
2. R. Xu, J. Chen, and S. Feng, *Stud. Surf. Sci. Catal.* **60**, 63 (1991).
3. S. Dhingra and R. C. Haushalter, *J. Chem. Soc., Chem. Commun.* 1665 (1993); I. D. Williams, J. Yu, H. Du, J. Chen, and W. Pang, *Chem. Mater.* **10**, 773 (1998) and references therein.
4. W. T. A. Harrison, T. E. Martin, T. E. Gier, and G. D. Stucky, *J. Mater. Chem.* **2**, 175 (1992).
5. M. Cavellec, D. Riou, C. Ninclaus, J. M. Greneche, and G. Férey, *Zeolites* **17**, 250 (1996); K. H. Lii, Y. F. Huang, V. Zima, C. Y. Huang, H. M. Lin, Y. C. Jiang, F. L. Liao, and S. L. Wang, *Chem. Mater.* **10**, 2599 (1998) and references therein.
6. S. Natarajan, S. Ayyappan, A. K. Cheetham, and C. N. R. Rao, *Chem. Mater.* **10**, 1627 (1998) and references therein.
7. D. M. Poojary, A. I. Bortun, L. N. Bortun, and A. Clearfield, *J. Solid State Chem.* **132**, 213 (1997); C. Serre and G. Férey, *J. Mater. Chem.* **9**, 579 (1999) and references therein.
8. Y. Zhang, A. Clearfield, and R. C. Haushalter, *Chem. Mater.* **7**, 1221 (1995); M. I. Khan, L. M. Meyer, R. C. Haushalter, A. L. Schweitzer, J. Zubieta, and J. L. Dye, *Chem. Mater.* **8**, 43 (1996).
9. R. C. Haushalter and L. A. Mundi, *Chem. Mater.* **4**, 31 (1992).
10. N. Guillou, Q. Gao, M. Nogues, R. E. Morris, M. Hervieu, G. Férey, and A. K. Cheetham, *C. R. Acad. Sci. Paris II, C* **2**, 387 (1999).
11. Q. Gao, N. Guillou, M. Nogues, A. K. Cheetham, and G. Férey, *Chem. Mater.* **11**, 2937 (1999).
12. I. Abrahams and K. S. Easson, *Acta Crystallogr. C* **49**, 925 (1993).
13. A. Daidouh, J. L. Martinez, C. Pico, and M. L. Veiga, *J. Solid State Chem.* **144**, 169 (1999).
14. A. Jouini, M. Dabbabi, and A. Durif, *J. Solid State Chem.* **60**, 6 (1985).
15. M. Dutreilh, C. Chevalier, M. El-Ghozzi, and D. Avignant, *J. Solid State Chem.* **142**, 1 (1999).
16. B. Elbali, A. Boukhari, J. Aride, and F. Abraham, *J. Solid State Chem.* **104**, 453 (1993).
17. K.-H. Lii, P.-F. Shih, and T.-M. Chen, *Inorg. Chem.* **32**, 4373 (1993).
18. F. Sanz, C. Parada, J. M. Rojo, and C. Ruiz-Valero, *Chem. Mater.* **11**, 2673 (1999).
19. R. H. Jones, J. M. Thomas, J. Chen, R. Xu, Q. Huo, S. Li, Z. Ma, and A. M. Chippindale, *J. Solid State Chem.* **102**, 204 (1993).
20. M. Estermann, L. B. McCusker, C. Baerlocher, A. Merrouche, and H. Kessler, *Nature* **352**, 320 (1991).
21. A. K. Cheetham, G. Férey, and T. Loiseau, *Angew. Chem., Int. Ed.* **38**, 3268 (1999).
22. R. E. Morris and S. J. Weigel, *Chem. Soc. Rev.* **26**, 309 (1997).
23. Software packages SMART and SAINT, Siemens Analytical X-ray Instruments Inc., Madison, WI, 1996.
24. SHELXTL, Version 5.1, Siemens Industrial Automation, Inc., Madison, WI, 1997.
25. H.-M. Lin and K.-H. Lii, *Inorg. Chem.* **37**, 4220 (1998).
26. P. B. Moore and T. Araki, *Am. Mineral.* **62**, 692 (1997).
27. M. L. F. Phillips, W. T. A. Harrison, G. D. Stucky, E. M. McCarron III, J. C. Calabrese, and T. E. Gier, *Chem. Mater.* **4**, 222 (1992).